ISBN: 978-3-95450-231-8 ISSN: 2673-5490 doi: 10.18429/JACoW-IPAC2023-TUPA086

A POSITRON SOURCE DEMONSTRATOR FOR FUTURE COLLIDERS

N. Vallis[1*], P. Craievich, R. Zennaro, M. Schaer,
B. Auchmann[2], M.I. Besana, M. Duda, R. Fortunati, H. Garcia-Rodrigues, D. Hauenstein,
R. Ischebeck, E. Ismaili, P. Juranic, J. Kosse, A. Magazinik, F. Marcellini, U. Michlmayr,
S. Muller, M. Pedrozzi, R. Rotundo, G.L. Orlandi, M. Seidel[1], M. Zykova,
Paul Scherrer Institute, Villigen, Switzerland
[1]also at EPFL, Lausanne, Switzerland
[2]also at CERN, Geneva, Switzerland

Abstract

Regarding high current e+ sources, the almost universal usage of target-based production schemes combined with conventional capture technology has led to poor transmission efficiencies. This long-standing difficulty to handle the extreme e+ transverse emittance and energy spread has been a major limitation for future, high luminosity lepton collider designs. The PSI Positron Production (P-cubed or P^3) experiment, framed in the FCC-ee study, is a demonstrator for a e+ capture system with potential to improve the state-of-the-art e+ yield by an order of magnitude. The experiment will be hosted at the SwissFEL facility at PSI as of 2025, where installation works are ongoing. This paper is an overview of P^3, with a particular focus on the novel capture system and associated e+ beam dynamics. A concept for the experiment diagnostics is also introduced.

INTRODUCTION

Efficient production and capture of high current positron (e+) beams are major enabling factors for future, high luminosity colliders such as FCC-ee [1]. The demanding electron and positron (e+e-) current requirements of FCC-ee rely largely upon the injector design [2], and more specifically on a e+ source based on the interaction a 6 GeV electron (e-) beam and a 17.5 mm-thick amorphous W target [3]. Previous FCC-ee studies show high e+ yields at the target, above 13 N_{e+}/N_{e-}[1]. However, due to the extreme transverse emittance and energy spread of the secondary beam [4], a conventional capture system based on a normal conducting (NC) flux concentrator will barely preserve a yield of 1.1 N_{e+}/N_{e-} at the the damping ring (DR), where e+ have their emittance cooled [3]. Based on a 3.2 GeV primary e- beam and a similar capture system, the state-of-the art of high yield e+ sources is that of SuperKEKB, with 0.5 N_{e+}/N_{e-} at the DR [5].

The PSI Positron Production (P^3 or P-cubed) experiment, whose layout is shown in Fig. 1, is a demonstrator for a new, highly efficient e+ source for FCC-ee. The P^3 e+e- beam will be generated according to parameters in Table 1. The novelty of the experiment lies in a highly efficient capture section based on a solenoid system featuring high-temperature superconductors (HTS) and two RF cavities with large aperture. In addition, the experiment diagnostics will be equipped for e+e- time structure, charge and energy spectrum measurements. P^3 will be installed at SwissFEL facility [6] at PSI as of 2025, ready for operation in early 2026.

Table 1: Primary e- of FCC-ee linac and SwissFEL

	FCC-ee [7]	P^3
Energy [GeV]	6	
σ_t [ps]	3.33	
σ_x, σ_y [mm]	0.5	
Target length [mm]	17.5	
Q_{bunch} [nC]	1.7 - 2.4	0.20[1]
Reptition rate [Hz]	200	1[1]
Bunches per pulse	2	1[1]

[1]Defined by radiation protection limitations at SwissFEL.

KEY TECHNOLOGY

Multi-Tesla solenoid fields around the production target are a widespread technique for e+ emittance matching [4]. The P^3 experiment is particularly ambitious, foreseeing fields of 12.7 T delivered through a HTS solenoid [8] made out of 5 non-insulated ReBCO [9–11] coils, and hosted at a Helium-free cryostat with two single-stage cryocoolers [12]. A prototype of the HTS solenoid was successfully assembled and tested at PSI, demonstrating Helium-free, conduction-cooled operation at 2 kA, generating a 18 T field on axis [13].

Capture and acceleration is provided by two S-band RF cavities of 1.2 m length, based on a novel approach standing wave solution of large iris aperture of 40 mm diameter to improve transverse acceptance. The frequency of 3 GHz corresponds to commercial S-band components. A double feeder coupler placed centrally will feed each cavity with the power from one single klystron, reaching a gradient of 18 MV/m. The cavities can reach 100 Hz repetition rates. RF phases be adjusted independently through an in-vacuum phase shifter developed in-house.

16 NC solenoids will surround the RF cavities. Fed with 220 A, they will deliver a uniform magnetic field of 0.45 T along the beam axis. The solenoids are winded in 22 layers and 12 helical windings per layer, with 3.5 mm diameter cooling water channels. Each device will be 112 mm long, with aperture and outer diameter 160 mm and 556 mm respectively.

* nicolas.vallis@psi.ch
[1] Ratio of surviving e+ and primary e-.

ISBN: 978-3-95450-231-8 ISSN: 2673-5490 doi: 10.18429/JACoW-IPAC2023-TUPA086

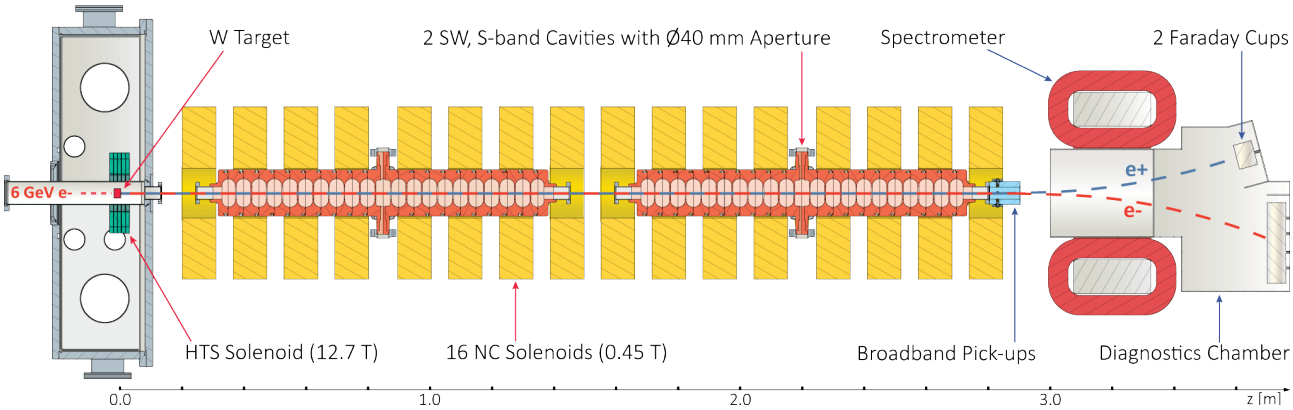

Figure 1: Layout of the P^3 experiment featuring key hardware components (red arrows) and diagnostics (blue arrows).

BEAM DYNAMICS[2]

The e+ production scheme described in Table 1 will generate a secondary e+ distribution of 2574 pC in the multi-MeV range, representing a yield of 13.85 N_{e+}/N_{e-} at the target exit face. Such e+ distribution will have a moderate beam size ($\sigma_x \approx 1$ mm) and bunch lentgh ($\sigma_t \approx 3.3$ ps), yet very high energy spread ($\Delta E_{RMS} \approx 115$ MeV) and transverse momentum ($\sigma_{px} \approx 8$ MeV/c).

Transverse Dynamics

The HTS and NC solenoid arrangement will provide an excellent e+ matching and confinement by making up an adiabatic matching device or AMD [14–16] based on a smooth, proportional to $1/z$ transition of the magnetic profile from the 12.7 T peak to the 0.45 T plateau. This technique will, in short, transform the e+ distribution at the target into a beam of large transverse size ($\sigma_x \approx 6$ mm) and moderate momentum ($\sigma_{px} \approx 2.5$ MeV) at the entrance of the 1st RF cavity. The magnetic channel created by NC solenoids will then confine the matched beam along the RF cavities, where maximum flatness and strength should be aimed for minimum e+ losses. In this sense, the 0.45 T field is high enough to provide high capture rates and avoid excessive cost and power consumption.

Longitudinal Dynamics

Under the influence of the 12.7 T solenoid field, newly generated e+e- will describe spiraling trajectories with a wide range of Larmor frequencies due to energy spread [4]. This will elongate the beam longitudinally and the RF cavities, as a consequence, will form consecutive e+e- bunches over many buckets, making the RF phase[3] choice vital for e+ transmission. A scan of the two RF phases is shown in Fig. 2, where two working points of interest were found, the first of which at Φ = (140,-80), providing a maximum captured charge of 1250 pC -or 6.25 N_{e+}/N_{e-}- in a region of on-crest acceleration, which tends to bunch e+ in the first RF bucket. A second working point at Φ = (70,-110) would provide a maximum yield of 4.64 N_{e+}/N_{e-} the FCC-ee DR[4] according to our estimations, by reducing the energy spread. Interestingly, this is achieved by e+ bunching in the second RF bucket through deceleration at the first cavity [19].

[2] All results are based on Geant4 [17] and ASTRA [18] simulations.
[3] No RF phase reference considered.
[4] Yield at DR estmation method in [8]

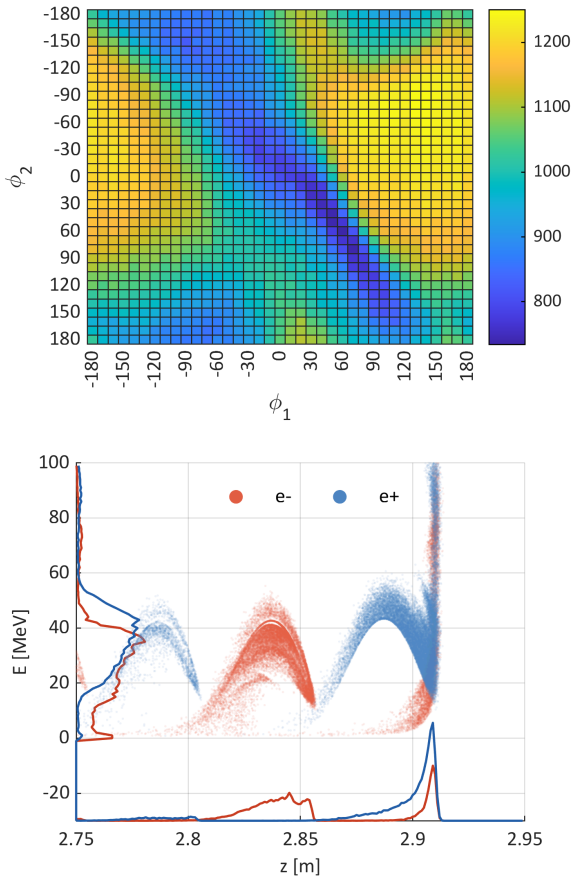

Figure 2: 2D RF phase scan of captured charge after 2nd cavity (top) and longitudinal profile of e+e- at maximum charge (140, -80) working point (bottom).

ISBN: 978-3-95450-231-8 ISSN: 2673-5490 doi: 10.18429/JACoW-IPAC2023-TUPA086

BEAM DIAGNOSTICS

A concept for the experiment diagnostics is shown in Fig. 3, featuring a sequence of tools before and after e+e- separation at the spectrometer.

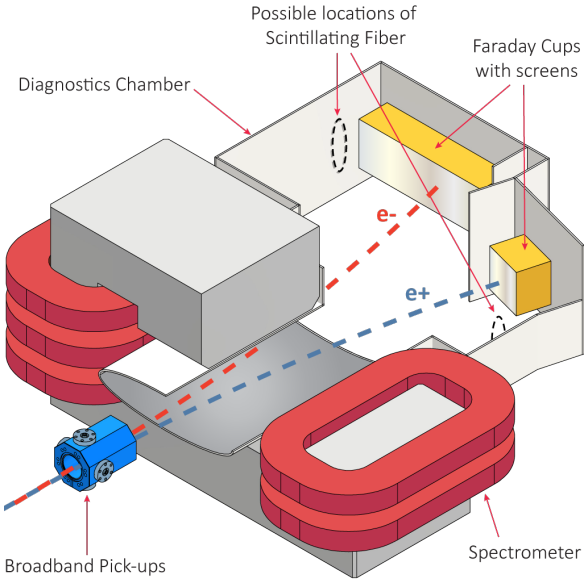

Figure 3: P^3 diagnostics setup.

Broadband Pick-ups

Four Broadband Pick-ups (BBPs) at the exit of the second RF cavity will measure the time structure of the captured e+e- beam before separation, including bunch-by-bunch measurements of charge and longitudinal bunch length. This technique is based on similar ultrafast pick-ups in current accelerator facilities [20–22]. In P^3, e+ and e- bunches after the 2nd cavity will have an RMS longitudinal length of 33 ps and will be 167 ps apart, namely half an S-band period (See Fig. 2). The basic principle of BBPs is to detect the wake voltage of such bunches with little distortion, which requires very broad frequency response. Two BBP assemblies have been developed for P^3 based on feedthroughs of 27 GHz [23] and 65 GHz [24], currently under fabrication. The signal acquisition will rely on a high-end oscilloscope of at least 10 GHz band and 40 GS/s sampling.

Faraday Cups

The spectrometer will divide the beam into two streams of e+ and e-, the charge of which is to be measured separately by two coaxial Faraday cups (FCs) arranged in a highly asymmetric setup. One FC of large transverse size (260x80 mm) will measure particles in a broad energy range (7-60 MeV), despite the significant horizontal dispersion introduced by the spectrometer due to energy spread. This FC is tuned at 12.5 Ω in pursuit of a minimum distance to the outer conductor, and matching to 50 Ω is achieved through an arrangement of four output coaxial connectors in parallel. A second FC of a more conventional 50 Ω impedance will detect particles in a 2.5-70 MeV spectrum by overlapping five separate measurements of concatenated energy ranges, through a scan of the spectrometer field strength. A simulation of such a measurement is shown in Fig .4, where the detected charge at Φ = (140,-80) is 1239 pC, showing a good agreement with the values in Fig. 2. The polarity of the spectrometer should be inverted for e+ and e- measurements with both FCs. The devices are based on 60 mm-thick Tungsten blocks supported by PEEK rods, providing a good frequency response up to 1 GHz.

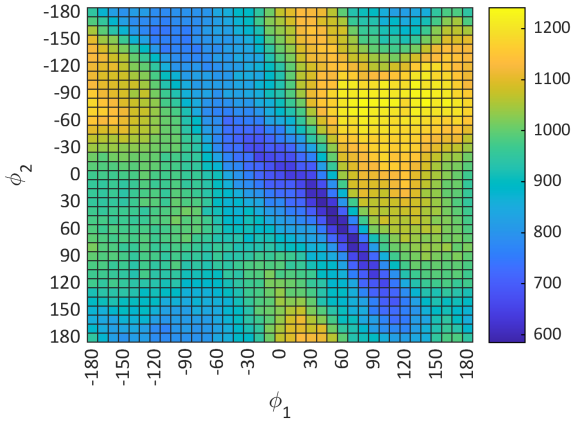

Figure 4: Simulation of captured charge measurement with 50 Ω FC during a 2D RF phase scan.

Scintillators in Diagnostics Chamber

The diagnostics chamber after the spectrometer will host at least two additional setups based on scintillator materials. First, the front face of the FCs will have scintillating screens [25] that will allow cameras mounted outside of the chamber to look at the e+ and e- signals, and see a rough energy spectrum. An alternate, high-resolution spectroscopic setup will be based on two pairs of scintillator fibers vertically oriented. Scintillator light will result from the ionization energy deposited by the intercepted charge and will be transmitted to a photomultiplier, whose analog readout will depict the relative energy distribution of the beams through a scan of the spectrometer strength.

CONCLUSION

An advanced version of the P^3 experiment was presented, including the final design of the capture section components with their most notable technical features, as well as a well-developed concept for the experiment diagnostics, equipped for both simultaneous and segregated detection of e+ and e- streams. Comprehensive simulation studies continue to suggest high potential to demonstrate a e+ yield one order of magnitude above the state of the art.

ACKNOWLEDGEMENT

This work was done under the auspices of the CHART Collaboration (Swiss Accelerator Research and Technology, `http://www.chart.ch`).

ISBN: 978-3-95450-231-8 ISSN: 2673-5490 doi: 10.18429/JACoW-IPAC2023-TUPA086

REFERENCES

[1] M. Benedikt, F. Zimmermann *et al.*, FCC-ee: the Lepton Collider. Future Circular Collider Conceptual Design Report Volume 2, *European Physical Journal Special Topics,* ***228(2)****, 261-623 (2019)* https://doi.org/10.1140/epjst/e2019-900045-4

[2] P. Craievich *et al.*, "The FCCee Pre-Injector Complex", in *Proc. IPAC'22*, Bangkok, Thailand, Jun. 2022, pp. 2007–2010. doi:10.18429/JACoW-IPAC2022-WEPOPT063

[3] I. Chaikovska *et al.*, Positron source for FCC-ee, in *Proc. IPAC'19, Melbourne, Australia* (JACoW, Geneva, Switzerland, 2019), pp. 424-427. doi:10.18429/JACoW-IPAC2019-MOPMP003.

[4] R. Chehab, Positron Sources, *in Proc. Cern Accelerator School, 5th general accelerator physics course, Jyvaskyla, Finland*, (CERN, 1994), pp. 2617-2620. doi:10.5170/CERN-1994-001.

[5] K. Akai, K. Furukawa and H. Koiso, SuperKEKB Collider, *Nucl. Instrum. Methods Phys. Res., Sect. A* ***907****, 188 (2018).* doi:10.1016/j.nima.2018.08.017

[6] E. Prat *et al*. A compact and cost-effective hard X-ray free-electron laser driven by a high-brightness and low-energy electron beam, *Nat. Photonics* ***14****, 748–754 (2020).* doi:10.1038/s41566-020-00712-8

[7] P. Craievich *et al.*, FCC-ee Injector Study and the P^3 Project at PSI, CHART Scientific Report (2022), https://chart.ch/wp-content/uploads/2023/02/FCCee-Injector-2022.pdf

[8] Y. Zhao, B. Auchmann, I. Chaikovska, R. Chehab, P. Craievich, S. Döbert,D. Duda, J. Kosse, A. Latina, P. Martyshkin, S. Ogur, R. Zennaro, Optimisation of the FCC-ee Positron Source Using a HTS Solenoid Matching Device, *in Proc. IPAC'22, Bangkok, Thailand* (JACoW, Geneva, Switzerland, 2022), pp. 2003-2006. doi:10.18429/JACoW-IPAC2022-WEPOPT062

[9] S. Hahn, D. K. Park, J. Bascunan and Y. Iwasa, HTS Pancake Coils Without Turn-to-Turn Insulation, in IEEE Trans. on Appl. Supercond., vol. 21, no. 3, pp. 1592-1595, June 2011, doi:10.1109/TASC.2010.2093492

[10] D. Hahn, K. Kim, H. Lee and Y. Iwasa, Current Status of and Challenges for No-Insulation HTS Winding Technique, *Teion Kogaku: Official Journal of the Cryogenic Association of Japan,* ***53(1)****, 2 (2018).* doi:10.2221/jcsj.53.2

[11] D.X. Fischer, R. Prokopec, J. Emhofer and M. Eisterer, The Effect of Fast Neutron Irradiation on the Superconducting Properties of REBCO Coated Conductors with and without Artificial Pinning Centers, *Supercond. Sci. Technol.,* ***31****, 044006 (2018)* doi:10.1088/1361-6668/aaadf2

[12] Sumitomo RDK500B, https://www.shicryogenics.com/product/rdk-500b-20k-cryocooler-series/

[13] M. Duda and J. Kosse, HTS solenoids for the PSI Positron production project in the context of the CHART FCCee injector study, Lecture at FCC Week (2022).

[14] R.H. Helm, Adiabatic Approximation for Dynamics of a Particle in the Field of a Tapered Solenoid, SLAC Report No. 4 (1962).

[15] R. Chehab, Positron Sources, *in Proc. Cern Accelerator School, 3rd general accelerator physics course, Salamanca, Spain*, (CERN, 1988), pp. 105-132, doi:10.5170/CERN-1989-005

[16] Y. Zhao *et al.*, Comparison of Different Matching Device Field Profiles for the FCC-ee Positron Source, *in Proc. IPAC'21, Campinas, SP, Brazil*, (JACoW, Geneva, Switzerland, 2021), pp. 2617-2620, doi:10.18429/JACoW-IPAC2021-WEPAB015.

[17] Geant4: Toolkit for the Simulation of the Passage of Particles Through Matter, https://geant4.web.cern.ch/

[18] ASTRA: A Space Charge Tracking Algorithm, url-https://www.desy.de/ mpyflo/

[19] B. Aune, R.H. Miller, New Method for Positron Production at SLAC, SLAC-PUB-2393, (1979).

[20] T. Suwada, M.A. Rehman, and F. Miyahara, First simultaneous detection of electron and positron bunches at the positron capture section of the SuperKEKB factory, *Sci. Rep.* ***11****, 12751 (2021)* doi:10.1038/s41598-021-91707-0

[21] T. Suwada, Direct observation of positron capture process at the positron source of the superKEKB B-factory, *Sci. Rep.* ***12****, 18554 (2022).* doi:10.1038/s41598-022-22030-5

[22] V. Arsov *et al.*, Evaluation of the cone-shaped pickup performance for low charge sub-10 fs arrival-time measurements at free electron laser facilities, *Phys. Rev. Accel. Beams* ***18****, 012801 (2012).* doi:10.1103/PhysRevSTAB.18.012801

[23] 27GHz SMA Feedthrough for UHV Applications 242-SMAD27G-C16, Allectra GmbH (2019).

[24] Microwave 1.85mm (SMA) feedthrough 242-SMAD65G-C16, Allectra GmbH (2022).

[25] C.D. Johnson, The development and use of alumina ceramic fluorescent screens, CERN Report No. CERN-PS-90-42-AR (1990).